9. V. I. Zinchenko and S. I. Pyrkh, "Calculation of a nonequilibrium viscous shock layer and associated heat exchange," Izv. Akad. Nauk SSSR, Mekh. Zhid. Gaza, No. 2 (1984).
10. A. M. Grishin, V. N. Bertsum, and V. I. Zinchenko, The Iterative-Interpolation Method and Its Application [in Russian], Tomsk. Gos. Univ., Tomsk (1981).
11. R. H. Feldhuhm, "Heat transfer from a turbulent boundary layer on a porous hemisphere," AIAA Paper No. 119 (1976).
12. V. V. Lunev, Hypersonics [in Russian], Mashinostroenie, Moscow (1975).
13. A. N. Lyubinov and V. V. Rusanov, Gas Flow Past Blunt Bodies [in Russian], Part 1, Nauka, Moscow (1970).
14. V. N. Kharchenko, "Heat exchange in a hypersonic turbulent boundary layer with insufflation of cooling gases through a crack," Teplofiz. Vys. Temp., No. 1 (1972).

INFLUENCE OF RAREFACTION ON THE UNSTEADY IMPINGEMENT PROCESS OF AN UNDEREXPANDED SUPERSONIC JET ONTO A PERPENDICULAR OBSTACLE

A. V. Savin, E. I. Sokolov,
V. S. Favorskii, and I. V. Shatalov

UDC 533.6.011.8

The destruction of a steady flow in front of an obstacle placed perpendicular to the axis of an underexpanded supersonic jet is one of the most interesting physical phenomena in jet flows. The essential feature of this is that a smooth quasi-steady variation of distance h from the nozzle to the obstacle or of the pressure ratio of the jet $n = p_a/p_\infty$, leads to a sudden discontinuous breakdown of the steady flow: a wave structure in front of the obstacle begins to oscillate with frequency of order several kilohertz (with nozzle exit diameter d_a = 10 mm), while the pressure at the obstacle varies with the same frequency. In contrast to jet noise with constant inflow, which has a broadband spectrum, in an enclosed space the acoustic field has clearly defined discrete frequencies.

At present, there are several hypotheses [1-4] concerning the source of these oscillations, which attests to the absence of a generally accepted theory. Also unclear is the cause of the sharp transition to unsteady impingement. In this situation, to create a conclusive theory of this process, we expand the range of parameters over which this phenomenon has been studied; this is as instructive for numerical modeling as for experiments. In particular, until now there has been almost no study of the influence of viscosity on the process of unsteady jet impingement. Experimental results of this investigation are given below.

1. The experiments were conducted in a vacuum chamber of volume 10 m^3 with pressure $p_\infty = 10^2$-0.1 Pa. To measure the pressure, mechanical gauges, U-shaped manometers and thermocouple vacuum gauges were used. The full-scale pressures ranged from 10^5-10^2 Pa, which allowed variation of the Reynolds number Re_* from 5×10^2 to 5×10^3 for Mach numbers M_a from 1 to 3.35 and $n \leq 500$. The working gases were air and helium at temperature T_0 = 293 K. The receiver with the nozzle and the obstacle were installed on three-axis translation stages. The indices 0, *, a, and ∞ refer to stagnation, sonic, nozzle exit and ambient conditions, respectively.

To measure the pressure fluctuations at the obstacle, type IS-2156 piezoelectric transducers were used. The diameter of the active transducer surface was 1.5 mm, while the characteristic dimension of the jet under study was 25-30 mm. The resonant frequency of this transducer is greater than 100 kHz, which allows measurement of frequencies up to 50 kHz. The nonuniformity of the resonant frequencies of the transducers was checked by comparing frequency spectra of each transducer with that of a capacitive microphone (Bruel and Kjaer, model 4135). The discrepancy in the readings was lower than 3 dB in the range 0-40 kHz.

Leningrad. Translated from Prikladnaya Mekhanika i Tekhnicheskaya Fizika, No. 6, pp. 78-83, November-December, 1991. Original article submitted January 22, 1990; revision submitted June 12, 1990.

0021-8944/91/3206-0893$12.50

In the experiments, frequency spectra were recorded as well as dependences of the integrated acoustic emission level and the fluctuating pressure at the obstacle while varying the nozzle position relative to the obstacle. The signal was processed using a set of apparatus (model 22E) from the East German company RFT.

The transducer signals were preamplified and input to a scaling instrument amplifier with variable gain. Low-frequency electrical interference was rejected with a high-pass filter. The frequency response of the transducer–preamplifier–scaling amplifier–filter circuit was flat to within ±3 dB in the range 0.15-20 kHz. The signal level at the filter output was monitored by the instrument described; from this output the signal was input to a sequential spectrum analyzer with frequency range 0.02-20 kHz.

To record the exterior acoustic emission under rarefied conditions, an electret microphone (MD-52B) with frequency response 0.1-20 kHz was used. The acoustic frequency and the frequency of pressure fluctuations at the obstacle were measured using a frequency meter (Ch3-33). Flowfield visualization was accomplished using a glow discharge. Data were recorded for a series of nozzle positions relative to the obstacle.

2. We analyze the characteristics of unsteady flows for finite, fixed Re_*. Figure 1 shows the acoustic levels (curve 1) and the fluctuating pressures at the edge and in the center of the obstacle (curves 2 and 3) for $M_a = 2$, $n = 13$, rarefaction parameter $Re_L = Re_*(p_0/p_\infty)^{-0.5} = 240$, $\gamma = 1.4$, $d_a = 5.2$ mm. The values of h and of the distance z from the jet axis in the plane of the obstacle are related to the quantity $d_a M_a \sqrt{\gamma n}$, which allows data for dense jets [2] to be generalized; $\Delta L = 20 \log(\langle p \rangle / p_f - L_w$. Here $\langle p \rangle$ is the root-mean-square pressure fluctuation at the obstacle, $p_f = 2 \times 10^{-5}$ Pa is the sound pressure at the audibility threshold, and L_w is the level of broadband background noise. Upon increasing h, the pressure fluctuation attains three peaks greater than 20-30 dB, with sharply defined edges; we can consider these the first, second and third unsteady regimes. The form of the fluctuation's dependence on h in the first and second regimes is analogous to that of the noise level in an acoustic field. The transition from the second regime to the third occurs abruptly and is accompanied by a decrease by 15-20 dB of the fluctuation at the obstacle center. At the obstacle edge, the fluctuations in the second and third regimes do not differ by much.

The distributions of pressure fluctuations over the obstacle for a given regime are shown in Fig. 2 (curves 1-12 correspond to h = 0.67, 0.72, 0.85, 0.94, 1.12, 1.23, 1.3, 1.43, 1.46, 1.65, 1.74 and 2.24). Before the start of the first regime with $h < h_{1H}$ (Fig. 2a), there is on the obstacle an annular band of increased (by 2-4 dB) pressure fluctuation, evidently corresponding to the region of closest approach of the mixing layer to the obstacle. At the onset of the first and second regimes, the fluctuation sharply increases, and on the edge it remains 8 dB higher than at the center (curves 1-8). Upon transition to the third regime, the form of the distribution changes (Fig. 2c). At the center, the fluctuation is close to zero, while at the edge it is higher than 22 dB, close to that of the second regime (curves 9-12).

Temporal scans of the pressure fluctuations at various points on the obstacle are given in Figs. 3-5 for the three unsteady regimes considered, for $M_a = 2$, $n = 13$, $Re_L = 240$, $\gamma = 1.4$, $d_a = 5.2$ mm and h = 0.9, 1.34 and 1.46 respectively. The distance z from the axis took the values 4.8, ±3.8, ±2.9, ±1.9, 1.0 and 0. For the first and second regimes, the pressure at the center varies regularly with significant amplitude (Figs. 3, 4). At the edges of the constant-fluctuation zone, the phase at all points on the obstacle is the same. After crossing the maximum (Fig. 2), another component is superposed on the signal, which gradually changes its form, and then its phase by 180°. At points symmetric to the axis, the pressures have the same phase, which confirms the conclusion of symmetrical, longitudinal oscillations in regimes I and II. The presence of additional signal components may be explained by perturbations occurring in the mixing layer beyond the triple point and breaking down the radial flow along the obstacle.

In the third regime (Fig. 5) the fluctuation amplitude at the center is low, while the frequency is double that of the sound in the exterior field. However, at the first measurement point where $z \neq 0$, the frequency is again the same as that of the exterior field, and the amplitude increases in comparison with the center. For increasing z, at the edges of the regime the phase of this signal changes slowly. Additionally, at symmetric points the phase shifts by 180° (Fig. 5, curves 1 and 2). Apparently, in this regime the elements of

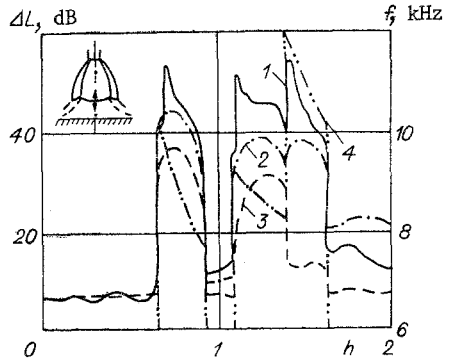

Fig. 1

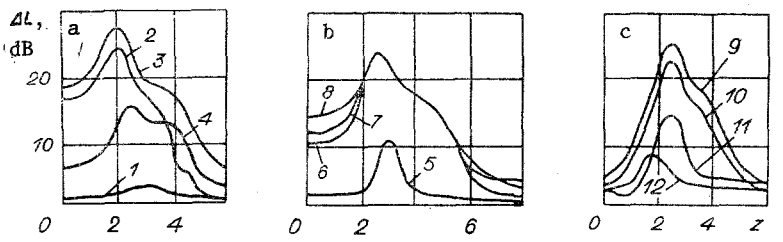

Fig. 2

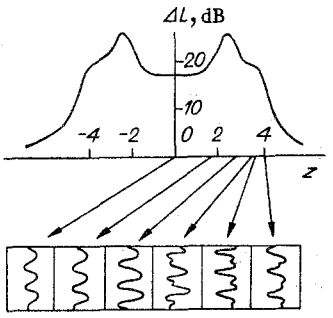

Fig. 3

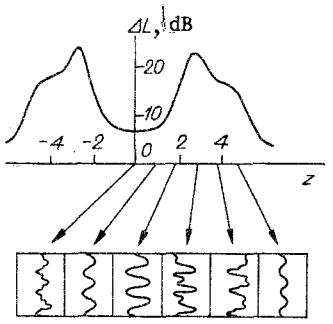

Fig. 4

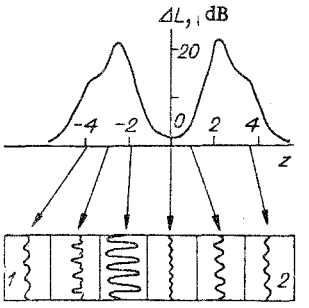

Fig. 5

the gasdynamic structure oscillate circularly, analogous to the behavior noted in [5], while the acoustic emission becomes spiral-shaped.

Recording of the acoustic frequency spectra using the microphone, installed in the chamber, showed that in the unsteady regimes there is one discrete component which exceeds the level of broadband noise by 30-45 dB and is clearly audible if the amplifier output is connected to a loudspeaker; a smooth translation of the obstacle gives rise to a sudden onset of sound. This fact, in combination with those previously given, verifies that the processes observed in the chamber are the same as those studied earlier under atmospheric conditions, where Re_* is higher by three orders of magnitude. The acoustic emission frequency is identical to that of the pressure fluctuations on the obstacle, which agrees with the conclusions of [2]. The dependence of the oscillation frequency f on h is shown by curve 4 of Fig. 1. For increasing h, the frequency of all three regimes decreases.

3. To investigate the influence of rarefaction on the unsteady impingement process, the jet Re_L was varied by proportional control of p_0 and p_∞. The latter was determined by the gas flow rate into the chamber.

The existence of clear limits of the unsteady regimes, noted in the present experiments, allows a quantitative estimate of the influence of Re_L on the flow. In particular, the experiments showed that the oscillation frequency in all three regimes does not depend on Re_L. This makes it possible, using similarity parameters [2] and taking into account the self-similarity of the longitudinal and lateral dimensions of the shock layer between the central shock and the obstacle from the quantity $d_a\sqrt{n}$, to express the process frequency measurements as a linear dependence

$$a_0/fd_a = K_1\Delta/d_a + K_2\sqrt{n}. \qquad (3.1)$$

with 20% accuracy or better. Here a_0 is the stagnated speed of sound, Δ is the time-averaged central shock-obstacle standoff, and the coefficients K are defined in Table 1. For their calculation, besides the results of the present work (about 40 measurements), data from [2] and [6] were used, encompassing the parameter range M_a = 1-3, n = 2-200, Re_* = 10^6-5 × 10^2 and γ = 1.25-1.67.

In Fig. 6 are shown the experimentally obtained limits of existence of the unsteady regimes for M_a = 2.12, n = 110, γ = 1.4 and d_a = 1.23 mm. The regions of existence of the

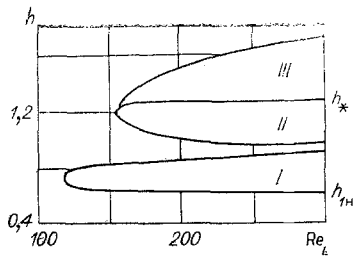

Fig. 6

TABLE 1

Regime number	K_1	K_2
I	4,1	0,6
II	1,9	0,1
III	0,75	1,0

TABLE 2

Regime number	Re_L^0 for M_a = 1	Re_L^0 for M_a = 2	Re_L^0 for M_a = 3
I	220	128	110
II	130	150	155
III	—	160	180

regimes are denoted respectively by I, II, and III. The values of h_{1H} and h_*, corresponding to the onset of the first regime and the transition to interaction of the second 'barrel' of the jet with the obstacle, are computed using the equations given in [7]. For high Re_L, the regime boundaries are practically independent of this parameter and are given by the empirical functions of [7]. With decrease of Re_L below 300, together with decrease of the pressure fluctuation amplitude, the range of distance h of existence of each of the three regimes shrinks. Further reduction of Re_L leads to sequential disappearance of the third, the second, and finally the first regime. For $M_a = 1$, decreasing Re_L causes the first regime to disappear, followed by the second, while the third is not observed.

The results obtained verify that the presence of unsteady regimes of the form observed here is connected with the existence of a shock-wave structure in the jet and its transformation with variation of Re_L. Thus, for $Re_L < 100$, corresponding to wash-out of the wave structure of the first barrel [8], the unsteady regimes are not seen for all values of the parameters. Fow inflow of an underexpanded rarefied jet with $M_a > 1$ on the obstacle, for $Re_L < 120$ a transition is possible from a central-shock structure (diagram of Fig. 1) to the so-called X-shaped configuration, which leads to the onset of on-axis regions of supersonic flow in front of the obstacle and a second shock wave. As a result, we find a regime of interaction with the undisturbed first barrel [9]. The transition to the X-shaped configuration is accompanied by disappearance of the second unsteady regime. The third regime is not seen under these interaction conditions.

The obtained data show that the onset of the unsteady regimes is possible only when Re_L exceeds some minimum Re_L^0. The values of Re_L^0 for all three regimes, as functions of M_a, are given in Table 2.

The decrease of Re_L^0 for increasing M_a of the first regime agrees with the results of [2], where it was established that the fluctuation amplitude increases with increasing M_a. The disappearance of the second and third regimes is connected with the decreasing diameter of the central shock density jump and the contracting lateral shock layer dimensions upon transition to the X-shaped shock wave configurations [9].

Increase of the pressure ratio, giving rise to a proportional increase in both longitudinal and lateral dimensions of the shock-wave structure, leads in accordance with (3.1) to a decrease of the fluctuation frequency, and has practically no effect on Re_L down to $n = 500$.

LITERATURE CITED

1. K. Merch, Theory of the Hartman Jet Generator [in Russian], Mekhanika, Moscow (1965).
2. B. G. Semiletenko, B. I. Sobkolov, and V. N. Uskov, "Approximate calculation of amplitude-frequency characteristics of unsteady interaction of a supersonic jet with a perpendicular flat obstacle," Izv. Sib. Otd. Akad. Nauk SSSR, Technical-Scienfic Series, No. 13, Issue 3 (1975).

3. V. N. Glaznev and V. S. Demin, "Semi-empirical theory of generation f discrete tones by a supersonic underexpanded jet impinging on an obstacle," Zh. Prikl. Mekh. Tekh. Fiz., No. 6 (1975).
4. V. G. Dulov, "A mathematical model of the oscillation cycle for unsteady interaction of a jet with an obstacle," Zh. Prikl. Mekh. Tekh. Fiz., No. 6 (1978).
5. G. V. Naberezhnova and Yu. N. Nesterov, "Unstable interaction of an expanding supersonic jet with an obstacle," Trans. TsAGI, Issue 1765 (1976).
6. A. V. Solotchin, "Concerning the instability of a supersonic underexpanded jet impinging on an obstacle," in: Gasdynamics and Acoustics of Jet Flows [in Russian], Nauka, Novosibirsk (1976).
7. E. I. Sokolov and V. N. Uskov, "Interaction of a supersonic axisymmetric jet with an obstacle and supersonic counterflow," in: Jets and Separated Flows [in Russian], G. G. Cherny, A. I. Zubkov, and M. M. Gilinskii, eds., Izd. Mosk. Gos. Univ., Moscow (1986).
8. V. V. Volchkov, A. V. Ivanov, N. I. Kislyakov, et al., "Low-density jet from a sonic nozzle with high-pressure Drop," Zh. Prikl. Mekh. Tekh. Fiz., No. 2 (1973).
9. E. I. Sokolov and I. V. Shatalov, "Flow similarity parameters for the interaction of a supersonic underexpanded jet on a perpendicular flat obstacle," in: Dynamics of Inhomogeneous and Compressible Media [in Russian], Izd. Leningr. Gos. Univ., Leningrad (1984).

CLOSURE OF THE EQUATIONS OF TURBULENCE USING THE ANALYTIC AND SCALING PROPERTIES OF THE SPECTRAL FUNCTIONS

S. R. Bogdanov

UDC 532.517

We discuss a spectral method of closing the equations of fully-developed shear turbulence based on the hypotheses of scaling invariance of the long-wavelength fluctuations of the velocity field and factorization of the dependence of the spectral functions on the magnitude and orientation of the wave vector k. It is also assumed that certain universal scaling functions appearing in the parametrization are analytic in k, rather than the individual components of the spectral tensors. It is shown that with these assumptions the turbulent structure is described locally by a small number of secular parameters, for which a relatively simple system of quasilinear differential equations is derived. In addition to the correlation length, mean rate of energy dissipation, and the Reynolds stress tensor (as in the semi-empirical models) the secular quantities also include the "fast" part of the pressure–deformation-rate correlation tensor, or equivalently the second orientation moments of the spectral function F_{ij}.

It was shown in [1] that the structure of fully developed isotropic turbulence produced by a grid in the long-wavelength region can be described by two secular fields: the mean rate of energy dissipation $\langle\varepsilon\rangle$ and the correlation length r_c.

The possibility of a simple description of this kind is intimately connected with the assumption that turbulent flow behaves as a critical system. The basis for this analogy is the similarity of the large-scale disturbances of the velocity field and the existence of a power-law (with exponent β) part of the spectrum in the inertial region. The intrinsic scales of length and time are the dissipative (Kolmogorov) quantities $r_d = (\eta^3/\langle\varepsilon\rangle)^{1/4}$ and $t_d = (\eta/\langle\varepsilon\rangle)^{1/2}$. The scaling dimensionality a of the velocity field in the approximation $\beta = 5/3$ is equal to 1/3, while the scaling dimensionality of the field ε in the same approximation is $(-\mu/2)$. Here μ is the spectral index characterizing energy dissipation fluctuations and η is the kinematic viscosity.

Petrozavodsk. Translated from Prikladnaya Mekahnika i Tekhnicheskaya Fizika, No. 6, pp. 83-93, November-December, 1991. Original article submitted June 6, 1989; revision submitted July 10, 1990.

0021-8944/91/3206-0897$12.50